

Solubility of iron in carbonic acid solutions

Cornelis de Waard,
Shell Research(retired), The Netherlands cdewaard@xs4all.nl

1. Abstract

From data in literature a model has been developed for the prediction of the concentration of dissolved iron, resulting from the corrosion of steel in carbonic acid. It explains the occurrence of iron carbonate supersaturation with the presence of an iron bicarbonate complex ion which increases the total dissolved iron concentration far above what is expected on the basis of the solubility product of iron carbonate only. This complex is formed in the corrosion reaction, but not, or very slowly, when FeCO_3 is dissolved in carbonic acid. The iron in this complex is chemically different from Fe^{2+} . The effect on corrosion rate prediction has been reviewed. The resulting model predicts the formation and breakdown of protective iron carbonate scale, and the effect of the presence of different levels of H_2S .

2. Introduction

The prediction of the concentration of dissolved iron in carbonic acid solution is of great practical importance, since its presence can reduce the corrosion rate of iron and steel equipment used for production and transport in oil and gas production. It increases the pH, and plays a role in the formation of protective scale. The Fe-concentration at saturation with FeCO_3 is predicted from the solubility product K_{spFeCO_3} , which is defined as the product of the activities of the ions concerned in a saturated solution. For low concentrations activities may be replaced by concentrations:

$$K_{\text{spFeCO}_3} = [\text{Fe}^{2+}]_{\text{at}} [\text{CO}_3^{2-}]_{\text{at}} \quad (1)$$

where $[\text{Fe}^{2+}]_{\text{sat}}$ is the concentration at FeCO_3 saturation for the equilibrium



When K_{spFeCO_3} is exceeded, iron carbonate should precipitate. The values for K_{spFeCO_3} as function of temperature correspond to very low iron carbonate solubilities. This solubility product is obeyed when solid FeCO_3 is dissolved in water. However, there appear to be instances where this is not obeyed: in these cases more iron stays in solution than is compatible with this solubility product¹. Significantly, from a corrosion point of view, this occurs when iron is dissolved, through corrosion or anodic stimulation, in a carbonic acid solution. The phenomenon is referred to as "supersaturation" of iron carbonate, and has been explained with slow kinetics of the precipitation of iron carbonate². In the present paper, however, an alternative explanation will be proposed, i.e. that part of the iron is dissolved as a complex ion.

Evidence for the existence of a dissolved iron bicarbonate complex has been found by Vilche, Arvia et al.^{3,4}, and the probable role of such a complex in explaining supersaturation has been pointed out earlier by de Waard and Lotz⁵.

A solution of Fe^{2+} in water consists of hydrated ions: $\text{Fe}^{2+}(\text{H}_2\text{O})_6$. There are two contributions to the bond between the ion and a the water molecules: Coulomb

attraction between the ion and dipoles induced in the water molecules, and dative covalent bonding⁶, where bonding electrons are all provided by the O-atoms in the coordinated water molecules (also called ligands).

The FeHCO_3^+ ion complex may be seen as a hydrated Fe^{2+} ion where one of the six coordinated water molecules has been replaced by a bicarbonate ion⁷. The Fe in this complex also shares electrons with O-atoms from the HCO_3^- ion, resulting in an ion with different chemical properties. The official name of this complex would be hydrocarbonatoferrate(II). In the present paper we will refer to this species as Ferrous Bicarbonate Complex or FBC. It may be possible that the Fe^{2+} ion can form complexes with more bicarbonate ions, but their stability is expected to be low because of the repulsive Coulomb forces between bicarbonate ions. For the present study, only the above FBC is taken into account.

Most analysis methods do not differentiate between dissolved Fe in such a bicarbonate complex and hydrated Fe^{2+} ions in a solution, which may explain the observed deviation from the solubility product. Many analytical techniques use complex-forming chemicals such as phenanthroline as a photometric indicator⁸, which forms a coloured complex with all Fe, and which will replace the bicarbonate complex. Also, chemicals are often added to samples to convert all dissolved iron to Fe^{3+} for colorimetric measurement with thiocyanide. In this way only a total iron concentration can be measured. In the following it is assumed that the actual Fe^{2+} concentration obeys the value derived from the solubility product K_{spFeCO_3} , and that the observed Fe surplus is caused by the presence of FeHCO_3^+ ions.

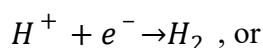
Other similar complexes like e.g. $\text{Fe}(\text{OH})^+$ can exist, but their concentration under pH conditions relevant to corrosion is probably so small that they can be ignored. Stability constants (= concentrations of complex divided by that of reactants) of such complexes have been reviewed by Fouillac and Criaud⁹, but reliable values are difficult to find.

3. Mechanism of Corrosion Reaction

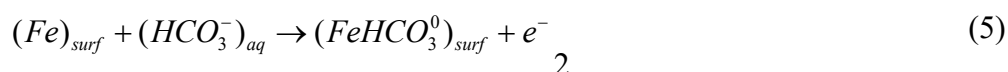
As stated in the introduction, supersaturation with dissolved iron is mainly observed when the dissolved iron originates from iron corroding in carbonic acid solution¹, but not when it originates from pure crystalline FeCO_3 . Supersaturation can also be observed by adding a dissolved Fe^{2+} salt to a carbonic acid solution to which NaHCO_3 is added^{10 11}. A possible explanation could be that Fe^{2+} ions first form and accumulate in the double layer at the metal surface, which then react with the bicarbonate ions. Alternatively, formation of FeHCO_3^+ can be the result of an electrochemical surface reaction of solid Fe with HCO_3^- , since this is the most abundant species¹² –apart from dissolved CO_2 – in the carbonic acid solution, e.g.:



together with a cathodic reaction e.g.



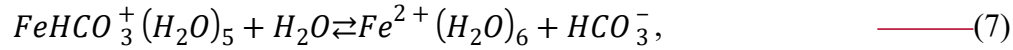
In this case the anodic dissolution could be initiated by a surface reaction step:



where the suffix *surf* relates to the metal's surface, and *aq* to the solution. The neutral ferrous bicarbonate complex on the metal's surface would then dissolve while releasing another electron:



This dissolved and hydrated complex ion will be in equilibrium with hydrated Fe^{2+} :



and when K_{spFeCO_3} is exceeded, solid $FeCO_3$ should precipitate.

As will be shown below, the above equilibrium is strongly on the side of the complex on the left, but shifts to the right with increasing temperature. If the $FeHCO_3^+$ ions in this case are also analysed as being Fe^{2+} , considerable "supersaturation" can be the result.

The fact that supersaturation does not occur when crystalline $FeCO_3$ is dissolved suggests that a slow dissolution step of the solid is rate controlling in that case.

4. Predictive model for $FeCO_3$ precipitation.

Referring to the above equilibrium (Eq. 7), the stability constant K_{FBC} of the Ferrous Bicarbonate Complex is defined as:

$$K_{FBC} = \frac{[FeHCO_3^+]}{[Fe^{2+}][HCO_3^-]} . \quad (8)$$

It is customary to leave out the H_2O molecules when referring to hydrated ions. When iron is dissolved by corrosion or anodic stimulation of a steel electrode in carbonic acid, the dissolved iron is distributed over FBC and Fe^{2+} in such a way that Eq. 8 is obeyed. The total dissolved iron concentration C_{Fe} , both as FBC and Fe^{2+} can then be written as:

$$C_{Fe} = [FeHCO_3^+] + [Fe^{2+}] = [Fe^{2+}](K_{FBC} \cdot [HCO_3^-] + 1) . \quad (9)$$

When $[Fe^{2+}]$ exceeds the saturation value $[Fe^{2+}]_{sat}$ dictated by the solubility product K_{spFeCO_3} of $FeCO_3$:

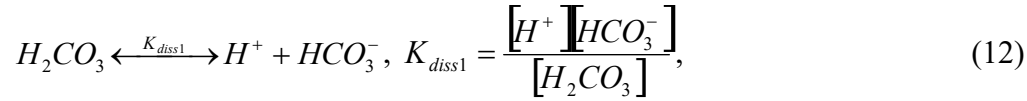
$$[Fe^{2+}]_{sat} = \frac{K_{spFeCO_3}}{[CO_3^{2-}]} , \quad (10)$$

precipitation of $FeCO_3$ will start. In terms of the total dissolved iron concentration C_{Fe} , this occurs when C_{FeSat} is exceeded:

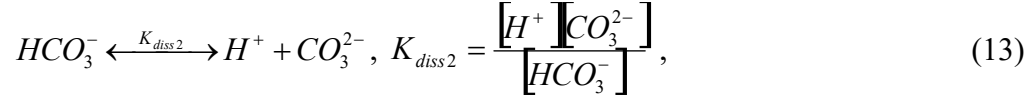
$$C_{FeSat} = \frac{K_{spFeCO_3}(K_{FBC} \cdot [HCO_3^-] + 1)}{[CO_3^{2-}]} . \quad (11)$$

Calculation of C_{FeSat} requires values for the temperature dependent equilibrium constants K_{spFeCO_3} and K_{FBC} as well as the concentrations of bicarbonate and carbonate ions, which are also pH dependent.

The concentrations of the carbonate and bicarbonate ions follow from:



and



Here $[H_2CO_3]$ represents the dissolved CO_2 concentration; the fact that most CO_2 is not present as carbonic acid, is accounted for in the values of the dissociation constants K_{diss1} and K_{diss2} . $[H_2CO_3]$ is constant at a given temperature and CO_2 partial pressure for the system under consideration ("open" system) and can be calculated from Henry's constant¹³ for CO_2 . In order to obtain C_{FeSat} , the pH at saturation has to be obtained with an iteration procedure described below in § 6.

5. Estimate of Stability constant for Ferrous Bicarbonate Complex

Dugstad measured the total dissolved iron concentrations obtained from corroding iron in CO_2 solutions at 20, 40, 60 and 80 °C as a function of time¹. Except for 20 °C, the iron concentrations decreased after some time, after reaching a maximum value. The 20 °C point was believed not to have reached this maximum, and was not used for the estimate. The other points represented supersaturation in terms of dissolved Fe by a factor 5-10. This decrease of the Fe concentration in the samples drawn from the CO_2 solutions is possibly caused by settling of some of the dispersed $FeCO_3$ precipitate on the steel coupon and the wall of the test vessel.

In order to obtain an estimate for K_{FBC} , the maximum Fe concentrations were taken to be the concentration where $FeCO_3$ precipitation started, i.e. a value for C_{FeSat} at these temperatures and pressures. Using the formula for K_{spFeCO_3} from Johnson et al², the Fe^{2+} saturation concentration at this point can be calculated by iterating over the pH to obtain $[CO_3^{2-}]$ at charge balance, while the $FeHCO_3^+$ concentration is obtained from $[total\ Fe] - [Fe^{2+}]$. By entering these concentrations in Eq.8, estimates of K_{FBC} at three temperatures can be obtained.

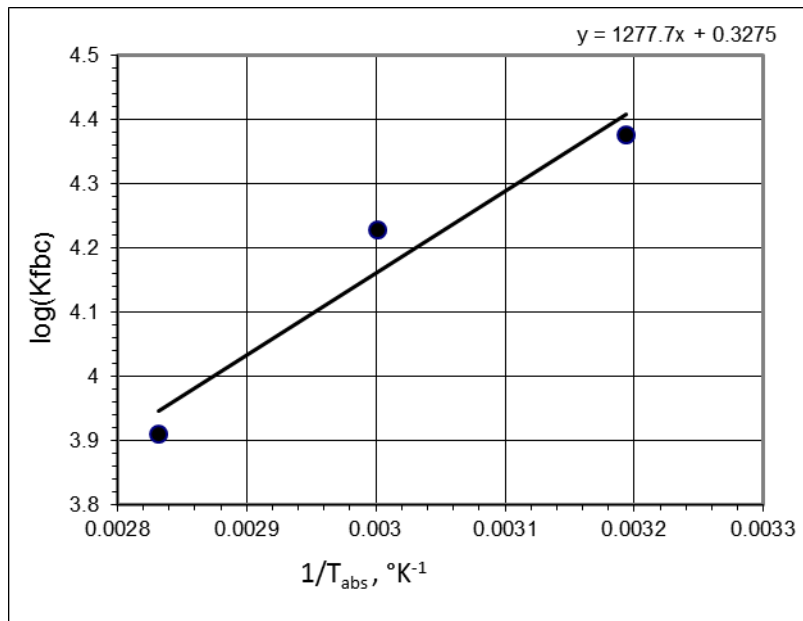


Fig.1. Arrhenius plot of K_{FBC} derived from Dugstad's experiments.

An Arrhenius plot of these values is shown in Fig.1, corresponding to the following dependence on temperature t :

$$\log(K_{FBC}) = \frac{1277.7}{t + 273.15} + 0.3275 \quad (14)$$

with $\log(K_{FBC}) = 4.51$ at 25°C .

The value presently estimated does not agree with the theoretically calculated value from Fouillac and Criaud⁹, which is much lower ($\log K_{FBC} \sim 2.1$). It may well be that their model for the complex on basis of Coulomb forces is not applicable, since the ligand is of the dative covalent type.

6. Results of model calculations

6.1 Total solubility of iron

When K_{FBC} is known, the calculation of the total solubility of iron for each temperature or CO_2 pressure can be done numerically, by iterating over the H^+ concentration until equilibrium of charge of Fe^{2+} , FeHCO_3^+ , H^+ , OH^- , HCO_3^- , CO_3^{2-} and HS^- –if H_2S is present– is achieved, while $[\text{Fe}^{2+}] = [\text{Fe}^{2+}]_{\text{sat}}$ (Eq.11).

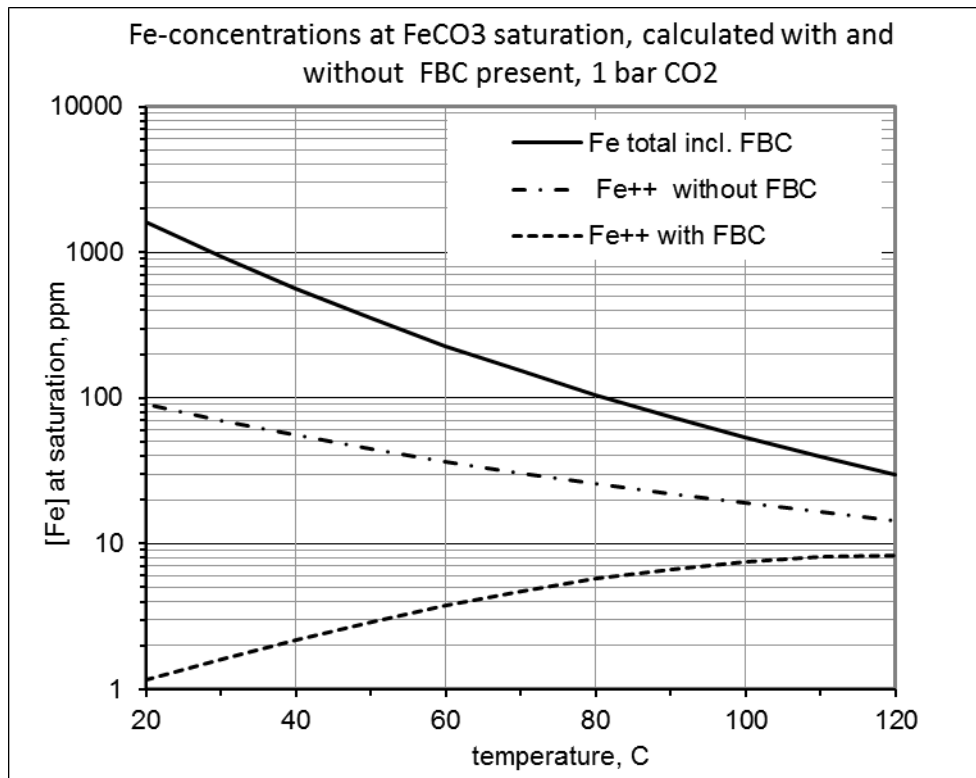


Fig. 2 . Total dissolved Fe concentrations at FeCO₃ saturation at 1 bar CO₂ as function of temperature, calculated with and without taking FBC into account.

Fig.2 gives an example of the results of this model for the concentrations of dissolved Fe²⁺ and FeHCO₃⁺ as a function of temperature at a partial pressure of CO₂ of 1 bar, when the solution is saturated with solid FeCO₃. In this figure is also shown the Fe²⁺ concentration which would be predicted from K_{spFeCO₃}, without the presence of the complex ion FBC. It follows that the latter would have to be exceeded substantially before precipitate is formed. The corresponding "supersaturation" (ratio of total [Fe]_{sat} × [CO₃²⁻] and K_{sp}) is shown in Fig. 3 as function of temperature; the calculated values are indeed in the range reported in literature¹⁰.

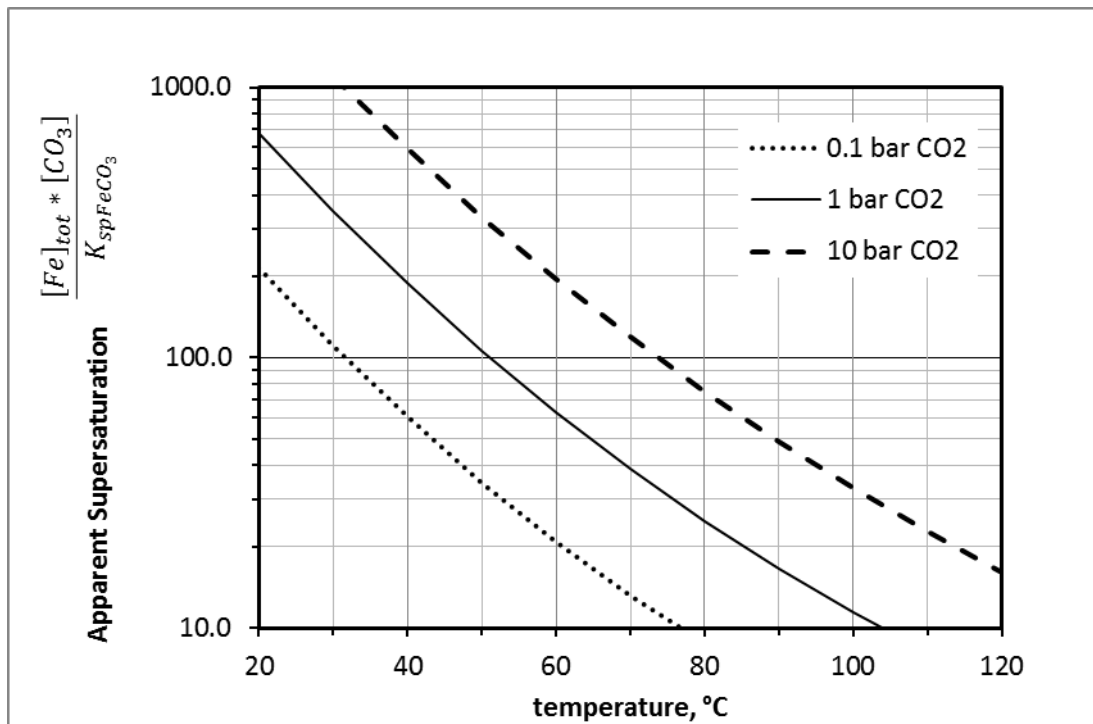


Fig. 3. Apparent supersaturation as function of temperature, calculated by taking the total dissolved Fe as being Fe^{2+} , at 1 bar CO_2 .

The large concentration of FBC at FeCO_3 saturation causes the pH to be higher than what would be predicted when only the Fe^{2+} concentration is taken into account, as shown in Fig.4. This causes the CO_3^{2-} concentration also to be higher than otherwise calculated, and consequently, the Fe^{2+} concentration is much lower.

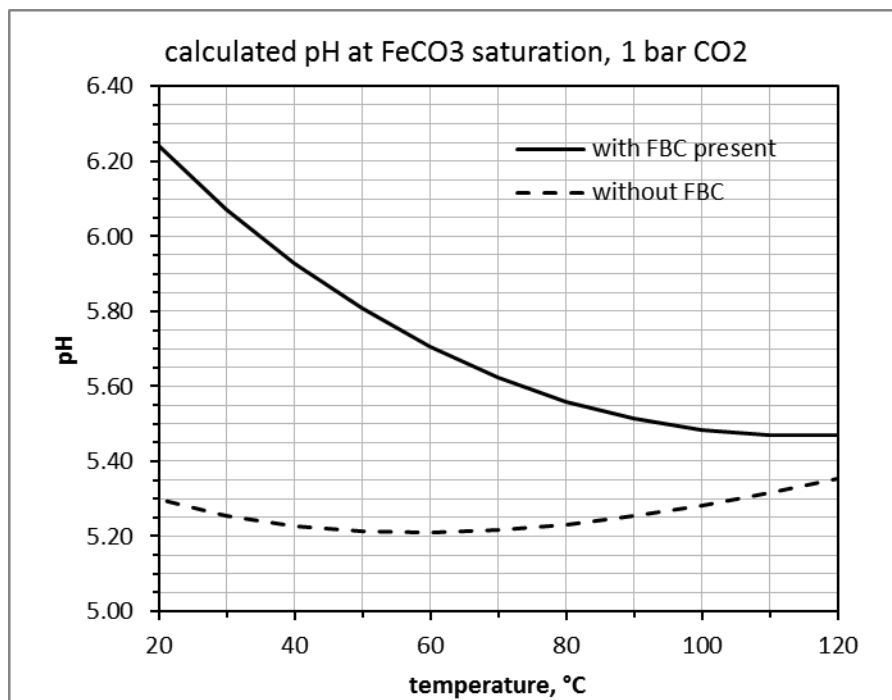


Fig.4. pH at FeCO_3 saturation as function of temperature.

6.2 Modelling corrosion rates and dissolved iron concentrations

CO₂ corrosion rates were calculated with empirical equations derived from a best fit to results of corrosion loop tests carried out at IFE, which was reported before¹⁴:

$$\log(V_r) = 4.84 - \frac{1119}{T} + 0.58 \log(pCO_2) - 0.34(pH_{actual} - pH_{CO_2}) \quad (15)$$

$$V_m = 2.8 \frac{U^{0.8}}{d^{0.2}} pCO_2 \quad (16)$$

V_r and V_m are associated with the reaction kinetics of the corrosion reaction (e.g. the charge transfer reaction) and with the mass transfer of the dissolved CO₂ from the bulk of the solution to the surface of the steel, respectively. They are combined to obtain the corrosion rate V_{cor} (mm/y):

$$\frac{1}{V_{cor}} = \frac{1}{V_r} + \frac{1}{V_m} \quad (17)$$

U is the liquid velocity (m/s), d is the internal pipe diameter (m).

In order to model the Fe concentration in a pipeline as a function of distance, the pipe length is divided into small sections Δx of, for example, 50 m, and for each section the pH is iterated in small steps. For each pH value the possible Fe²⁺ and FeHCO₃⁺ concentrations are calculated from the charge resulting from all other ion concentrations, using Eq.'s 9-13. Assuming steady state, a mass balance for [Fe²⁺] was then made for each pH, similar to the work by van Hunnik et al.¹⁵ The pH where the sum of in- and outflow, corrosion and precipitation of Fe²⁺ as FeCO₃ is zero then represents the steady state for that pipe section. The amount Q_{prec} of Fe²⁺ precipitated as FeCO₃ per second in each segment was calculated from:

$$Q_{prec} = ([Fe^{2+}] - [Fe^{2+}]_{sat}) \times Waterflowrate \quad (18)$$

when this is > 0. This implies the simplifying assumption that, at saturation, solid FeCO₃ is formed as fast as Fe²⁺ is generated. Work by Yang Yang¹⁰ has shown that the amount of precipitated FeCO₃ on a vibrating Fe-coated crystal indeed reacted immediately when the environment was changed, the change being complete after about one hour in this case. In terms of intended life of equipment, this is relatively fast.

6.3 Stability of Protective Scale

When precipitation of FeCO₃ occurs, the precipitate may form in the bulk of the solution, and on the corroding steel's surface. This may result in passivity¹⁶. According to Wei Sun¹⁷, however, the resulting layers can be quite porous. Prediction of the degree of protection this provides for the steel is difficult¹⁸. Later work¹⁰ showed that once the layer is formed, removal by flow is very difficult, unless the pH is lowered. At 80 °C this happened at a pH =5.8, at an apparent supersaturation of 10-20, while the present model predicts 5.7 at SS=18. Another approach has been the use of a scale factor, a multiplier for the corrosion rate which reduces corrosion when the so-called scaling temperature is exceeded.¹⁹ For the present predictive model for pipeline corrosion, it is assumed that when FeCO₃ precipitates, a protective layer is

always formed after some time, even with slow precipitation kinetics.

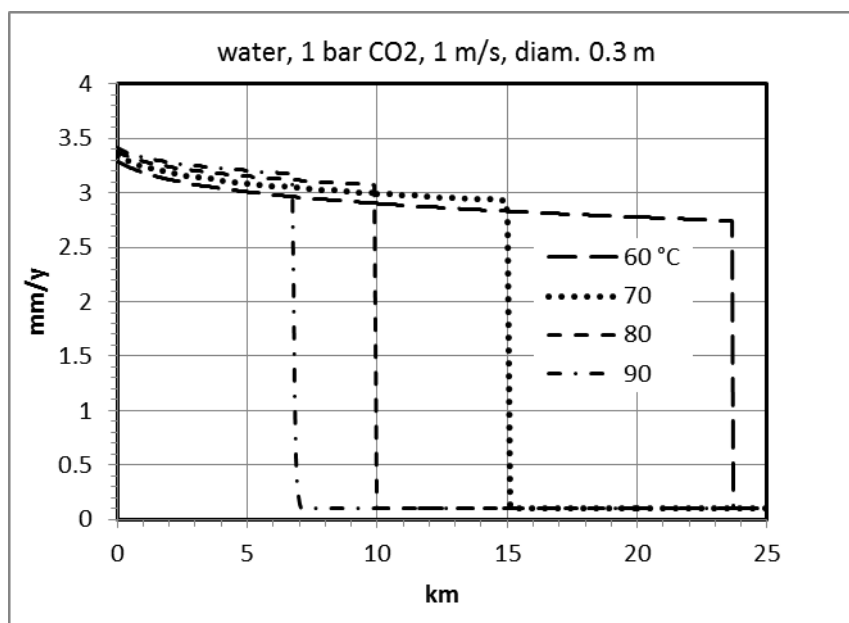


Fig. 5. Example of effect of temperature on formation of protective FeCO_3 layer.

The protective properties of a FeCO_3 layer are the result of an equilibrium between corrosion of unprotected areas, and precipitation and removal of FeCO_3 by the flowing liquid, which is difficult to model. Until more exact data become available, we have set the remaining corrosion rate with such a layer equal to 0.1 mm/y, because this was approximate rate found by Dugstad¹ at the end of his experiments, when the precipitate layer was fully established. Yang Yang¹⁰ also observed this corrosion rate when the layer was established. Similarly, the corrosion rate in the presence of a FeS layer was arbitrarily set to 0.01 mm/y for the purpose of this study, being the order of magnitude for the lowest rates found by Wei Sun¹⁷.

The effect of temperature on the formation of a protective layer is demonstrated in Fig. 5. Although the sharp dip in corrosion rate is probably not realistic, this demonstrates the increased tendency to form a scale with increasing temperature and prolonged exposure, as often observed in laboratory tests. In the slow precipitation model^{2, 15} a supersaturation threshold is used to predict protective layer forming.

The above result gives a possible explanation for the scale factor¹⁹ often used to estimate the effect of protective precipitates forming at temperatures above 60 °C. This factor was mainly based on average corrosion rates in stirred vessel exposure tests, or in circulating test loops. When a steel sample is exposed to carbonic acid while the FeCO_3 concentration increases as a result of corrosion, the sample may develop a protective layer for part of the exposure time, with a much smaller corrosion rate. The average corrosion rate is then a function of the exposure time –or the length of the pipe– involved. With the present model, however, the application of such a factor is no longer necessary, while it also gives the possibility to estimate the location where protective scale can be formed.

As expected, the model predicts that the addition of alkaline chemicals shifts the point where the layer is formed to the left. Also the presence of dissolved iron from other sources than corrosion will promote the formation of protective scale.

6.4 Effect of temperature gradient

When there is a temperature gradient along a pipeline, caused by cooling with distance, breakdown of a protective layer can occur. The total amount of dissolved iron needed for precipitation of FeCO_3 , and for formation/maintenance of a protective layer, is larger than hitherto thought because of the presence of FBC, and increases with decreasing temperature (Fig. 2).

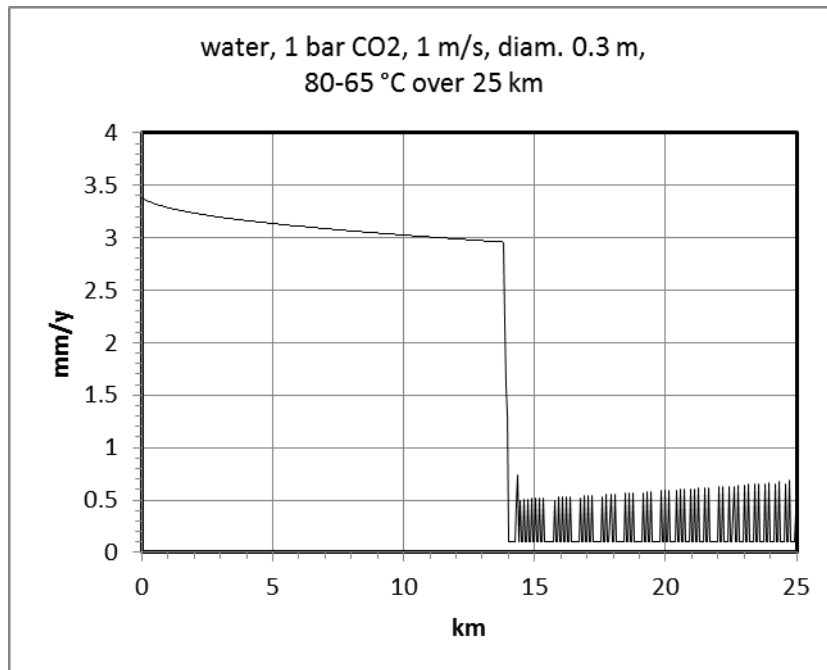


Fig. 6. Effect of a linear temperature profile, $0.6\text{ }^{\circ}\text{C}/\text{km}$, showing loss of stability of the FeCO_3 layer.

This can lead to a situation downstream of a FeCO_3 -layer where precipitation no longer occurs, and isolated patches of corrosion can then initiate.

If the amount of dissolved iron which is generated here, is high enough, a protective carbonate layer might be formed again further downstream. Such a situation is demonstrated in Fig. 6. The peaks shown reflect the average corrosion rate over the length of an element, in this example 50 m. Their height is limited to the rate needed to achieve FeCO_3 saturation in each pipe section. When Δx is too large, the peaks fuse together to a higher corrosion rate.

It should be noted that for the calculations with this model, the conservative assumption is made that dispersed FeCO_3 precipitate does not redissolve further downstream, because its dissolution rate is low.

Although it is not claimed that size and location of corroded areas in a pipeline can be exactly predicted, this shows a vulnerability of protective scale which has not been, to our best of knowledge, noted before. It may also be one of the underlying reasons for the localised corrosion often observed with CO_2 . Changes in (partial) CO_2 pressure resulting from pressure drop in gaseous systems can cause similar effects.

6.5 Effect of H_2S

When H_2S is present in sufficient concentration in addition to CO_2 , FeS can precipitate and form a protective layer. For a given CO_2 pressure, the concentration of dissolved iron needed for this is lower than that required for a FeCO_3 layer to develop. Fig. 7 demonstrates the effect on the corrosion rate of adding various

quantities of H₂S to 1 bar of CO₂, at 60 °C.

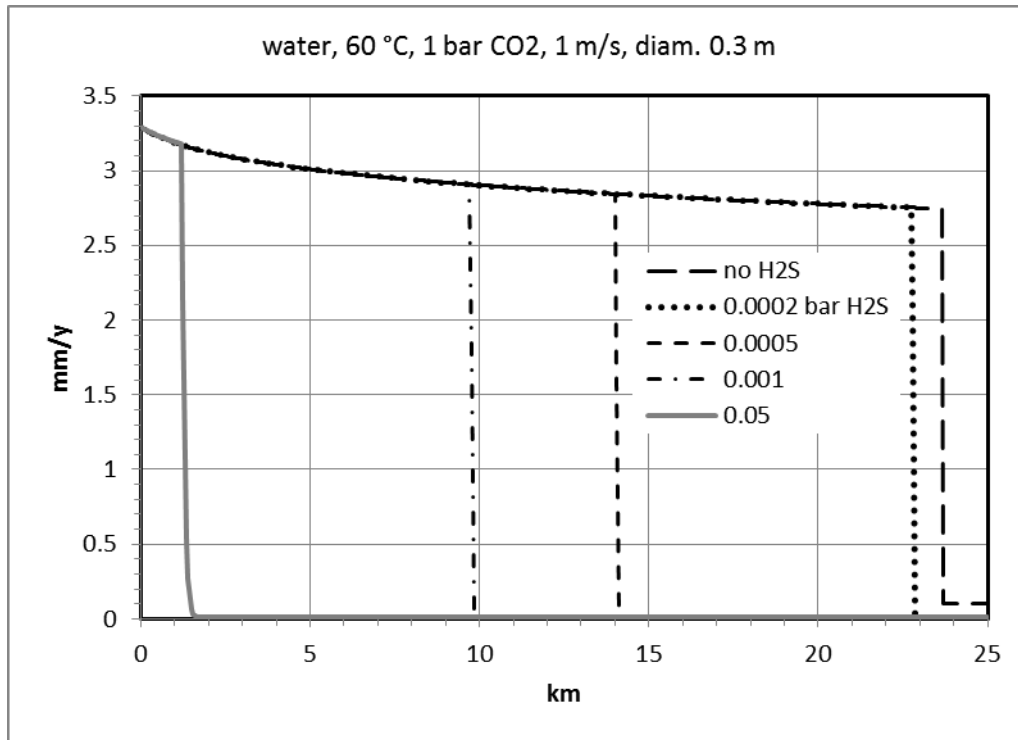


Fig. 7. Example of effect of H₂S partial pressure on the location where scale can be formed. Water, 60 °C, pipe diameter 0.3 m, 1 bar CO₂, 1 m/s.

For modelling purposes the proposal by Wei Sun¹⁷ was followed to use an expression for the solubility limit of FeS based on the HS⁻ concentration rather than that of S²⁻:



$$\text{with } K_{spFeS} = \frac{[Fe^{2+}][HS^-]}{[H^+]} \quad , \quad (20)$$

This was done because of the many uncertainties in the value of the equilibrium constant for the second dissociation step of H₂S.

The solubility of FeS is very small, and would result in a very small Fe²⁺ concentration, but the presence of CO₂ causes FBC to be in equilibrium with this Fe²⁺, and considerable "supersaturation" can occur. It should be appreciated that Fe²⁺ in H₂S solutions can also form numerous complex ions, which may by itself also lead to some supersaturation¹⁷.

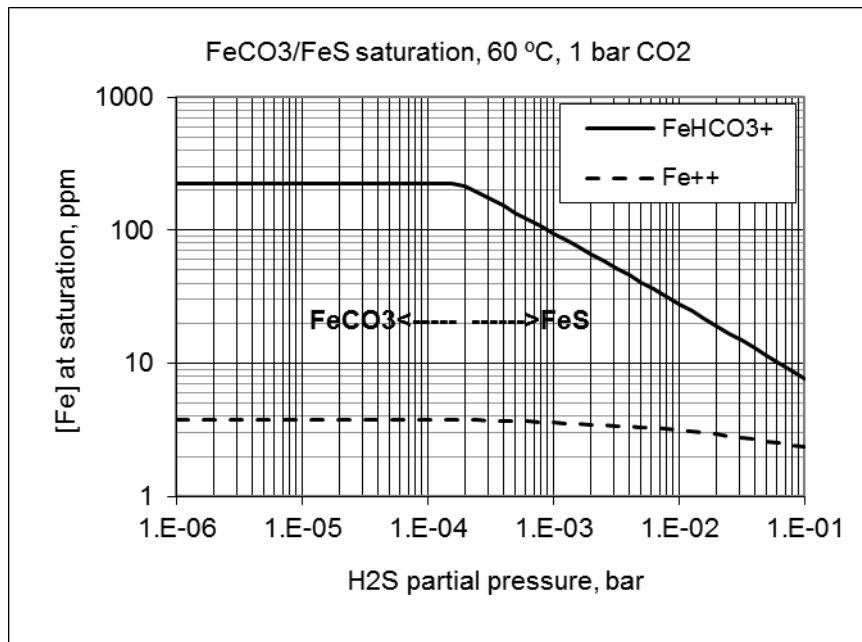


Fig. 8. Example of change from carbonate to sulphide precipitation by changing H₂S partial pressure, at constant CO₂ pressure of 1 bar, at 60 °C.

When both CO₂ and H₂S are present, their relative pressures determine the kind of scale that will be formed. In Fig.8 the Fe²⁺ line at the bottom of the graph represents the solubility limit, first determined by FeCO₃, but at 0.0002 bar H₂S this changes to FeS, which at that point has the smallest solubility. This suggests that either FeCO₃ or FeS is precipitated. This corroborates the work of Wei et al.²⁰, who found a mixed precipitate to be very rare. The ratio of pH₂S/pCO₂ at this point (~200 ppm) is in the same order of magnitude as that from work by Nestic²¹ and Pots²², and was found not to vary much with CO₂ pressure or temperature. At H₂S levels higher than this, in a FeCO₃ saturated solution, the precipitation of a protective FeS layer starts. The small concentration of Fe²⁺ in equilibrium with solid FeS is then still in equilibrium with an appreciable FBC concentration, as long as CO₂ is present. With 1 bar CO₂, at temperatures above 80 °C, and pH₂S~0.1 bar, the influence of FBC disappears.

Similar to the effect shown in Fig. 6., also here the protective FeS scale can be at risk when the fluid cools: when CO₂ is present, the amount of FBC in equilibrium with Fe²⁺ needed for precipitation of FeS or FeCO₃ would increase, and this could cause loss of protective scale and induce localised corrosion (Fig. 9). It was found that increasing the level of H₂S decreases the height of the peaks, but a minimum pH₂S has to be exceeded. Furthermore, the peaks are very near to each other, and sometimes occur in "patches".

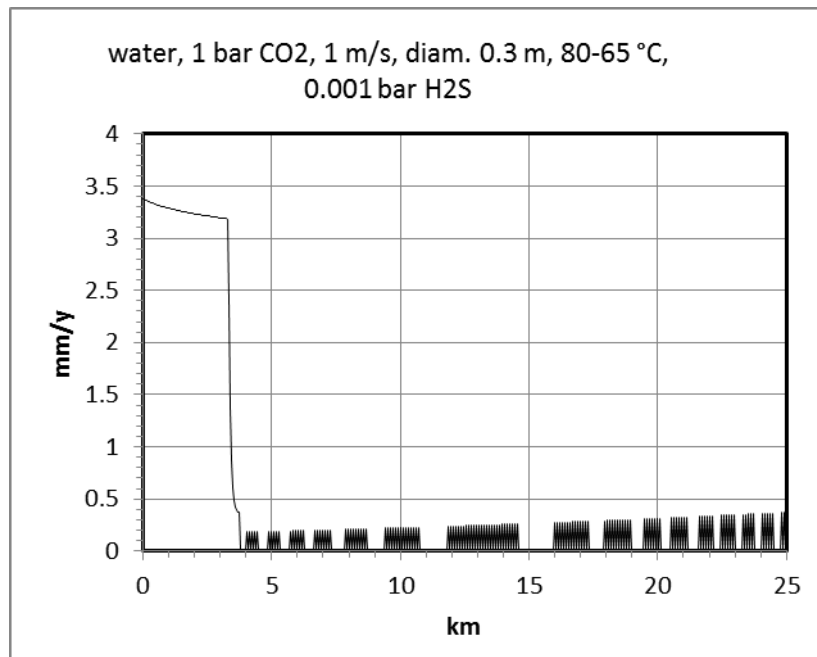


Fig. 9. Effect of a linear temperature profile, temperature gradient 0.6 °C/km, showing loss of stability of the FeCO_3 layer in the presence of 0.001 bar H_2S .

7. Conclusions

1. By taking into account the presence of a ferrous bicarbonate complex ion in equilibrium with dissolved ferrous carbonate, several hitherto unresolved issues in CO_2 corrosion can be understood.
2. The presence of this complex ion causes the total amount of dissolved iron to be much higher than would be expected from consideration of the iron carbonate solubility product only, since most analysis methods do not distinguish between the complexed iron and Fe^{2+} .
3. The presence of FBC can also explain in a comprehensive model the initiation of scale formation at higher temperature, and the potential for the protective scale breakdown as function of a temperature or pressure gradient along a pipeline.
4. The same comprehensive approach can incorporate the effect of H_2S in reducing corrosion rates, but with, similarly, a possible risk of pitting in a pipeline. The tendency for formation of iron carbonate or iron sulphide scale has been shown to be predictable from the ratio of H_2S to CO_2 .
5. The stability constant K_{FBC} estimated from Dugstad's data¹ is rather uncertain, which is not surprising in view of the small database. The value of K_{FBC} is also dependent on the value used for K_{spFeCO_3} in the interpretation of these data, the solubility product of FeCO_3 , which has been reviewed by Wei Sun¹⁷, while the use of activities rather than concentrations in the calculations could also further improve the model.

8. References

- ¹ A. Dugstad, "The importance of FeCO_3 supersaturation on the CO_2 corrosion of carbon steels", NACE CORROSION 92, paper 14.
- ² M.L. Johnson and M.B. Tomson, "Ferrous Carbonate Precipitation Kinetics and Its Impact on CO_2 corrosion", NACE CORROSION 91, paper 268.
- ³ C.R. Valentini, C.A. Moina, J.R. Vilche and A.J. Arvia, "The electrochemical

behaviour of iron in stagnant and stirred potassium carbonate-bicarbonate solutions in the 0-75 °C”, Corros. Sci. 25, 985 (1985)

⁴ E. Castro, J.R. Vilche and A.J. Arvia, "Iron dissolution and passivation in K₂CO₃-KHCO₃ solutions: Rotating ring disc electrode and XPS studies", Corros. Sci. 32(1), 37-50 (1991)

⁵ C. de Waard and U. Lotz, "Prediction of CO₂ corrosion of carbon steel", NACE CORROSION 93, paper 69.

⁶ Clark gives an excellent overview of complex ligands on internet:

<http://www.chemguide.co.uk/inorganic/complexions/whatis.html>

⁷ V.L. Snoeyink, D. Jenkins, "Water Chemistry", John Wiley & Sons 1980, p.200 e.v.

⁸ Belcher, R. "Application of Chelate Compounds in Analytical Chemistry", Pure and Applied Chemistry, 1973, volume 34, pages 13-27.

⁹ C. Fouillac and A.Criaud, "Carbonate and bicarbonate trace metal complexes, critical reevaluation of stability constants", Geochemical Journal, 18, 297 (1984)

¹⁰ Yang Yang, "Removal Mechanisms of Protective Iron Carbonate Layer in Flowing Solution", Dissertation Ohio University, August 2012

¹¹ Wei Sun and Srdjan Nestic, "Basics revisited: Kinetics of iron carbonate scale precipitation in CO₂ corrosion", NACE CORROSION 2006, paper 06365

¹² see e.g. Wikipedia.org/wiki/carbonic_acid

¹³ J.N.Butler, "Carbon Dioxide Equilibria and their applications", Addison-Wesley, 1982

¹⁴ C. de Waard, U. Lotz and A. Dugstad, "Influence of Liquid flow velocity on CO₂ corrosion: a Semi-Empirical model", by NACE Corrosion 95, paper no. 128.

¹⁵ E.W.J. van Hunnik, B.F.M. Pots and E.L.J.A. Hendriksen, "The formation of protective FeCO₃ corrosion product layers", NACE CORROSION 96, paper 6.

¹⁶ K.Videm, A.M.Koren, "Corrosion, Passivity and Pitting of Carbon Steel in aqueous solutions of HCO₃⁻, CO₂ and Cl⁻.", CORROSION/92, Nashville, paper 12.

¹⁷ Wei Sun, "Kinetics of iron carbonate and iron sulfide scale formation in CO₂ /H₂S corrosion", Dissertation Ohio University, November 2006.

¹⁸ M. Nordsveen, S. Nestic, R. Nijborg and A. Stangeland, "A Mechanistic model for carbon dioxide corrosion of mild steel in the presence of protective carbonate films – Part.1, Theory and verification”, Corrosion Vol. 59, no. 5, p.443

¹⁹ C. de Waard, U. Lotz and D.E.Milliams, "Predictive model for CO₂ corrosion in wet natural gas pipelines”, NACE CORROSION 91, paper 577.

²⁰ W. Sun, S. Nestic, and S. Papavinasam, "Kinetics of Iron Sulfide and Mixed Iron Sulfide/Carbonate Scale Precipitation in CO₂/H₂S Corrosion”, NACE Corrosion/2006 Conference, paper #644, Houston, USA, 2006

²¹ B. Brown, K.-L. Lee and S. Nestic, "Corrosion in Multiphase Flow Containing Small Amounts of H₂S”, NACE Corrosion/2003 Conference, paper #341, Houston, USA, 2003.

²² Pots, B. F. M., John, R.C., et al, "improvements on de-Waard Milliams Corrosion Prediction and Applications to Corrosion Management", Paper #02235, CORROSION/2002.